Focusing of Acoustic Energy at the Conical Point in Zinc

Kwang Yul Kim,[(1)] Wolfgang Sachse,[(1)] and Arthur G. Every[(2)]
[(1)]*Department of Theoretical and Applied Mechanics, Thurston Hall, Cornell University, Ithaca, New York 14853*
[(2)]*Department of Physics, University of the Witwatersrand, Johannesburg, South Africa*
(Received 22 February 1993)

This paper reports observations of the intense focusing of acoustic energy that occurs along the symmetry axis in a zinc single crystal. The focusing is associated with a conical point in the wave surface and thereby the phenomenon of external conical refraction. Our observations have been obtained with (i) pointlike piezoelectric transducers (PZT) as source and detector, (ii) a focused pulsed laser source and small PZT detector, and (iii) a breaking capillary source and capacitive detector at epicenter.

PACS numbers: 62.65.+k, 43.35.+d, 62.30.+d

The focusing of acoustic energy in elastically anisotropic solids has been widely studied with both thermal phonons and ultrasonic waves. Most investigations in the past have involved the use of phonon imaging, which displays the directional dependence of ballistic heat flux at cryogenic temperatures [1]. Scattering is much less an obstacle at ultrasonic frequencies where the attenuation is orders of magnitude smaller, and recently several authors [2–4] have reported the observation of focusing of ultrasonic waves at room temperature in cubic crystals and fiber composites.

There is an abundance of experimental observations of the focusing of phonons and elastic waves in cubic media and also to a lesser extent in trigonal and tetragonal media. However, no experimental observation of focusing in hexagonal media has been reported to our knowledge. Filling this gap is all the more important in view of the fact that a certain category of hexagonal crystals possesses an extraordinarily singular and degenerate type of focusing. This focusing is concentrated in the vicinity of an isolated point caustic located in the direction of a conical point in the wave surface, and it is closely associated with the phenomenon of external conical refraction. The condition on the elastic constants for the existence of this conical point is [5,6]

$$(C_{13}+C_{44})^2/[C_{13}(C_{33}-C_{44})] > 1 .$$

Every [6] has predicted the form of the unfolding of this point caustic into a connected pattern of line and cusp caustics when the symmetry is lowered.

This paper reports convincing evidence for the experimental observation of focusing of quasitransverse (QT) modes in a hexagonal zinc crystal. The zinc crystal specimen is disk shaped with a diameter of 75 mm and 25.8 mm thick. It is oriented in the symmetry [0001] direction, which is the direction of the point caustic for the QT modes in zinc [5]. The focusing of the QT modes will be discussed from two points of view. One is the theory of phonon focusing which is based on geometrical acoustics [7] and which deals with the directivity of the energy flux associated with a given distribution of wave normals $\hat{\mathbf{k}}$ which is often but not always taken to be isotropic. The other is a more rigorous approach based on the dynamic Green's function G_{33} for the medium [8–10], which incorporates the effects of both focusing and source directivity, and is not limited to the extreme far field. The subscript 3 in G_{33} refers to the symmetry direction. Because of the dominant effect of focusing, both methods will be shown to explain satisfactorily the experimentally observed focusing of QT waves in zinc near the symmetry axis.

We have used three methods to observe this focusing: first, pulsed excitation by a fixed longitudinal (L) mode piezoelectric transducer and detection with an L mode piezoelectric transducer (PZT) which is scanned across the face opposite to the source; second, excitation by irradiation with a scanned pulsed laser beam and detection using a fixed L mode PZT on the opposite side to the laser source; third, excitation by capillary fracture on the surface of a specimen and detection with a capacitive displacement sensor located at the epicenter. The size of all the sources and detectors is no greater than 1 mm in diameter except the L mode PZT sensor of diameter 1.3 mm for the detection of the laser generated ultrasound. The frequency bandwidth of the entire experimental system extends from 20 kHz to 2 MHz for the system using the piezoelectric transducer and from 10 kHz to 10 MHz in the case of the capillary fracture source and capacitive transducer. We have also observed the focusing of QT modes by adopting combinations of miniature shear/longitudinal piezoelectric transducers and shear/shear piezoelectric transducers, which essentially act in both cases as point-source/point-detection. Basically no additional information is obtained with these other combinations. Since the former three methods are easier to perform and they provide distinctive representations of the QT mode focusing, we concentrate solely on them in this paper.

Figure 1(a) shows the (010) section of the slowness surface of zinc. It consists of three sheets, belonging to the quasilongitudinal (QL), pure transverse (PT), and QT modes. In the figure [0001] is simply written as [001] and it represents the axis of transverse isotropy for zinc, and hence all such zonal sections are identical. In any zonal section the QL and QT waves are sagittally polarized while the PT waves are shear horizontally (SH)

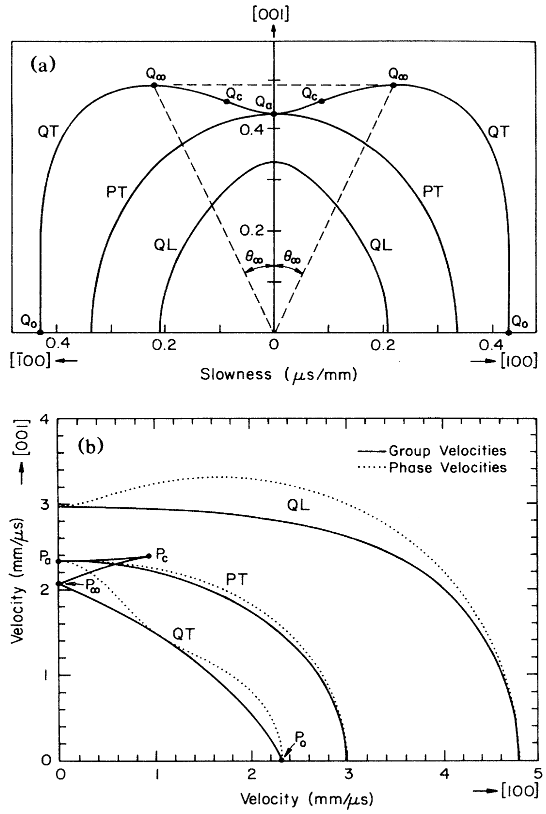

FIG. 1. (a) (010) section of the slowness surface in zinc. (b) (010) section of the group and phase velocity surfaces in zinc.

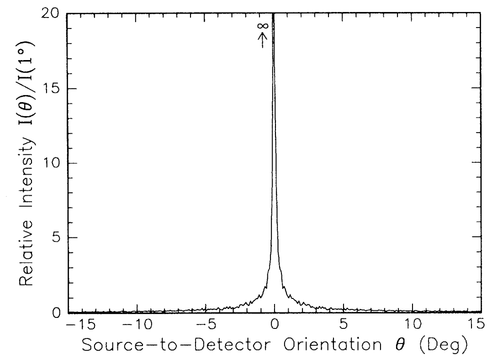

FIG. 2. Calculated QT mode focusing intensity $I(\theta)$ normalized with respect to $I(1°)$ in zinc.

polarized. The corresponding group velocity (or ray) surface is shown by the solid lines in Fig. 1(b). The values of elastic constants of zinc used to generate Figs. 1(a) and 1(b) are: $C_{11}=163.75$ GPa, $C_{12}=36.28$ GPa, $C_{13}=52.48$ GPa, $C_{33}=62.93$ GPa, and $C_{44}=38.68$ GPa. These are the values we obtained by measurement. The cuspidal feature shown in Fig. 1(b), which lies at 21.5° to the symmetry axis, is explicable in terms of the shape of the QT sheet of the slowness surface. Near the symmetry axis it is concave, with both principal curvatures being negative. At Q_c the principal curvature in the zonal plane changes sign, and between here and the point Q_∞ the surface is saddle shaped. At Q_∞ the principal curvature transverse to the zonal plane changes sign and beyond this point the slowness surface is convex in shape. There is a band on either side of the basal plane near Q_0 where the in-plane curvature of the slowness surface is again negative, but none of our observations relates to this region, and we will not discuss it any further. The gradient at a point on the slowness surface indicates the direction of energy flux or group velocity, which at the point Q_∞ is parallel to the symmetry direction [0001]. In Fig. 1(b) the points P_a and P_∞ on the symmetry axis, P_c on the cuspidal edge, and the point P_0 on the basal plane correspond to the points Q_a, Q_∞, Q_c, and Q_0 in Fig. 1(a), respectively. For simplicity of nomenclature, let us call the ray branches of the QT mode between P_a and P_c, P_c and P_∞, and P_∞ and P_0 by their acronyms, FQT (faster QT) mode, IQT (intermediate QT) mode, and SQT (slower QT) mode, respectively. Because of rotational symmetry the ray surface near P_∞ is conical in shape. All QT modes with their $\hat{\mathbf{k}}$ vectors lying on the circular cone generated by rotating $0Q_\infty$ around the symmetry axis have the same ray vector located at the conical point P_∞ and have their acoustic energy directed along the symmetry direction [0001]. This phenomenon is termed *external conical refraction* [11] for the reason that when this single QT ray impinges on the boundary between this hexagonal medium and an isotropic medium, the constituent vectors on being refracted in accordance with Snell's law emerge in the external medium as a family of rays lying on the surface of a cone.

Because of the axisymmetric nature of the sources and detection methods in our experiments, PT modes, being SH polarized, are neither generated nor detectable, and only QL and QT modes are observed. The focusing of the QL modes is insignificant, because their sheet of the slowness surface is everywhere convex [12] and so there is no folding of the wave surface [refer to Fig. 1(b)]. In what follows we confine our attention to the QT modes which exhibit strong focusing. A parameter that provides a good measure of focusing is the Maris phonon enhancement factor [7] A, which is given, in terms of the Gaussian curvature $K=L_1L_2$ of the slowness surface, where L_1 and L_2 are the two principal curvatures, the group velocity V, and the slowness s, by

$$A^{-1}=s^3V|K| .$$

Figure 2 shows the normalized focusing intensity $I(\theta)/I(1°)$ of QT waves in the top surface region with latitude θ less than 15° from the symmetry direction. It has been generated with a source at origin on the bottom surface using a Monte Carlo method, and is based on the assumption of a uniform distribution of $\hat{\mathbf{k}}$ in all directions.

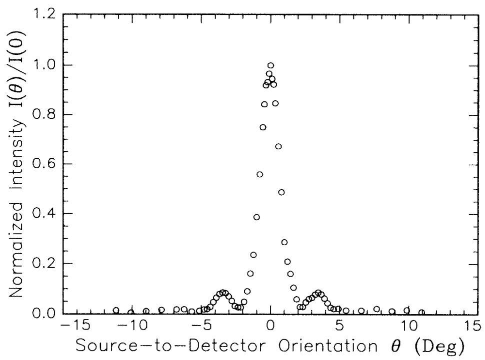

FIG. 3. Observed QT mode focusing pattern with L piezoelectric source and L piezoelectric detector.

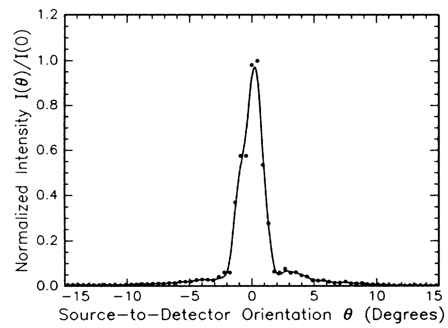

FIG. 4. Observed QT mode focusing pattern with laser source and L piezoelectric detector.

The intense central peak (whose intensity is theoretically infinite) corresponds to the conical direction P_∞ in Fig. 1(b) and also to the circle of zero Gaussian curvature on the slowness surface passing through the point Q_∞, on which A is infinite. Figure 2 shows how the QT acoustic intensity diminishes rapidly with increasing angular deviation from the symmetry axis.

Figures 3 and 4 show the angular variation of the normalized intensities obtained in two of our experiments. Both figures show that strong focusing is confined within an angle of about 1° of the symmetry direction. This is remarkable, considering the various factors that contribute to the widening of the focal region, including the finite size of source and detector and finite bandwidth of the source-generation–wave-detecting system. Figure 3 has been obtained with a combination of a longitudinal PZT source transducer fixed at the center of the bottom surface and an L mode PZT detector which scans across the epicentral position on the top surface, while Fig. 4 has been similarly determined by scanning a pulsed laser beam across the epicentral position on the top surface and using an L mode PZT detector fixed at the center of the bottom surface for detection. In both figures the square of the peak amplitude immediately following the QT mode arrival is used as a measure of intensity. Some of the detected wave forms on which Fig. 3 is based are displayed in Fig. 5. Both piezoelectric and laser excitations are axisymmetric and are expected to yield a ϕ-independent distribution of wave normals, where the angle ϕ denotes the longitude measured from the [100] axis. Figures 3 and 4 are consistent with the strong focusing of QT ultrasonic waves along the symmetry direction, which is predicted by the theory of phonon focusing.

In addition, Fig. 3 exhibits small secondary maxima at the source-to-receiver orientation of 3.5°. These secondary maxima are barely visible in Fig. 4. These secondary peaks arise from interference between the IQT and SQT wave branches, and occur at the positions predicted for a frequency of approximately 1.9 MHz, which is the dominant frequency in our signals. The unfolding of phonon focusing caustics into diffraction patterns at finite frequency was originally predicted by Maris [13] and has recently been observed by Hauser, Weaver, and Wolfe [3]. Further details on the nature of the diffraction pattern near the symmetry axis of zinc will be provided elsewhere.

Focusing of acoustic energy is not confined to quasiharmonic signals. It is a general feature of wave forms produced by time-dependent pointlike forces. It is particularly accentuated at wave fronts propagating the response to discontinuities in force, impulses, and other singular events, which are dominated by high frequency Fourier components. Analytical solutions for the full Green's function tensor along the zonal axis in an unbounded transversely isotropic medium and the epicentral component for an elastic half space have been obtained by Payton [9]. Figure 6 shows his calculation of the normalized displacement along the symmetry direction in units of $\rho F_3/(4\pi h C_{44})$ at a buried epicentral point due to an excitation of a Heaviside step source acting in the same direction. Here, ρ, F_3, and h represent the density of zinc, the magnitude of the Heaviside step force, and the distance from the source to the detector, respectively. The theoretical plate epicentral response would be similar to the half-space response, differing only in amplitude in accordance with the reflection coefficient of the traction-free surface until the arrival time of the 3L ray, which travels 3 times between the top and bottom surfaces of

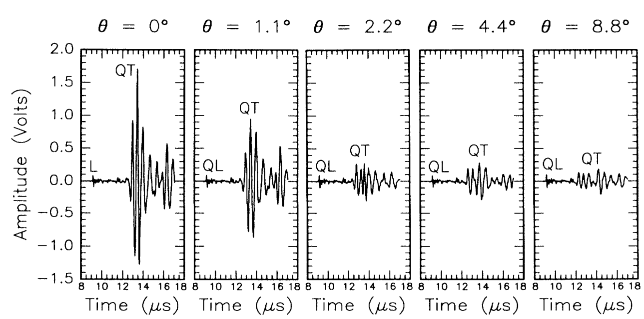

FIG. 5. Observed wave forms obtained with L piezoelectric source and L piezoelectric detector near the symmetry direction.

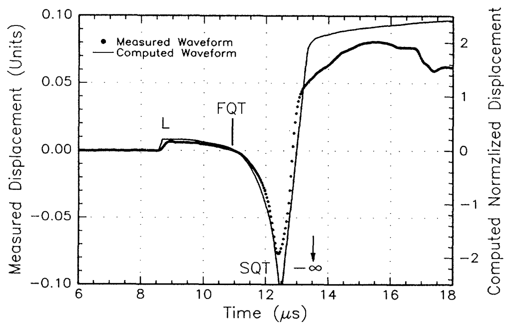

FIG. 6. Comparison between theoretical and observed epicentral displacements in the (0001) oriented zinc crystal.

the plate.

Comparison between theory and experiment is provided in Fig. 6, which also displays the epicentral displacement detected by a capacitive transducer of 1 mm diameter when a glass capillary of size less than 0.1 mm is broken on the surface of the zinc specimen by pressing the sharp edge of a razor blade down on it. The capillary fracture represents an axisymmetric acoustic emission source, the time function of which resembles a Heaviside step with rise time less than 0.1 μs [14]. The miniature capacitive transducer used in this experiment is described by Kim *et al.* [15]. The arrivals of L, FQT, and SQT rays are marked in the figure. Note close similarity between the two wave forms in Fig. 6. A discrepancy that sets in after 16 μs is due to the presence in the experimental curve of reflections from the side wall of the finite specimen. Payton's calculation predicts a change in slope in the wave form at the FQT wave arrival and a negative reciprocal square root singularity at the SQT wave arrival. The singularity is the result of the strong focusing of QT rays at the conical point in zinc. The measured epicentral wave form of Fig. 6 shows a deep negative minimum at the time of the SQT wave arrival very clearly. The finite value of the negative minimum in Fig. 6 is due to the finite size of the detector and finite bandwidth of the source-generation–wave-detection system. Away from the symmetry direction the negative singularity is weakened to a logarithmic divergence, which follows the IQT wave branch. Our measurements show a marked decrease in the depth of the minimum away from the symmetry axis. There is a second minimum which appears, being small to start with and growing in magnitude with increasing θ. It is associated with the arrival of the head wave which slightly precedes the arrival of the SQT ray. The evolution of the wave form with increasing θ and the changes that take place as the cuspidal edge is crossed will be described elsewhere. We emphasize that Fig. 6 includes the combined effect not only of focusing but also of the more gently varying anisotropic distribution of wave normals caused by the unidirectional nature of the force and detector directivity, both of which point in the symmetry direction. Comparison of Figs. 2–4 with Fig. 6 suggests that although the source and detector influence the detected amplitude of the QT mode propagating in the symmetry direction, the amplitude of this wave is mainly affected by focusing which is inherent to the propagation medium.

In conclusion this paper demonstrates the intense focusing of QT modes along the symmetry axis of zinc by various experimental methods. The experimental observations are consistent with the predictions both of the theory of phonon focusing and of theoretical Green's functions. Detailed experimental observations and theoretical calculations of the Green's function for a general direction will be published elsewhere.

The authors are grateful for the financial support of the Office of Naval Research. We are also thankful to Mr. B. F. Addis for growing a fine quality zinc crystal.

[1] See for a review, G. A. Northrop and J. P. Wolfe, in *Nonequilibrium Phonon Dynamics*, edited by W. E. Bron (Plenum, New York, 1985), p. 165.

[2] A. G. Every, W. Sachse, K. Y. Kim, and M. O. Thompson, Phys. Rev. Lett. **65**, 1446 (1990).

[3] M. R. Hauser, R. L. Weaver, and J. P. Wolfe, Phys. Rev. Lett. **68**, 2604 (1992).

[4] K. Y. Kim, A. G. Every, and W. Sachse (to be published).

[5] A. K. McCurdy, Phys. Rev. B **9**, 466 (1974).

[6] A. G. Every, Phys. Rev. B **34**, 2852 (1986).

[7] H. J. Maris, J. Acoust. Soc. Am. **50**, 812 (1971).

[8] A. N. Ceranoglu and Y. H. Pao, ASME J. Appl. Mech. **48**, 125 (1981); **48**, 133 (1981); **48**, 139 (1981).

[9] R. G. Payton, *Elastic Wave Propagation in Transversely Isotropic Media* (Martinus Nijhoff, Hague, 1983).

[10] A. G. Every, K. Y. Kim, and W. Sachse, in Proceedings of the Twenty-Ninth Winter School in Theoretical Physics, Karpacz, Poland, edited by T. Paszkiewicz and K. Rapcewicz (Plenum, New York, to be published).

[11] M. J. P. Musgrave, *Crystal Acoustics* (Holden-Day, San Francisco, 1970).

[12] G. F. D. Duff, Philos. Trans. R. Soc. London A **252**, 31 (1960).

[13] H. J. Maris, Phys. Rev. B **28**, 7033 (1983).

[14] F. R. Breckenridge, C. E. Tschiegg, and M. Greenspan, J. Acoust. Soc. Am. **57**, 626 (1975).

[15] K. Y. Kim, L. Niu, B. Castagnede, and W. Sachse, Rev. Sci. Instrum. **60**, 2785 (1989).